MODELLING OF THE LOW-PRESSURE GAS INJECTOR OPERATION

Dariusz SZPICA, Michał KUSZNIER

Faculty of Mechanical Engineering, Bialystok University of Technology, ul. Wiejska 45C, 15-351 Białystok, Poland

d.szpica@pb.edu.pl, michal.kusznier@gmail.com

Abstract: In recent years, there has been a growing interest in alternative sources of power supply for internal combustion engines. Lique-fied petroleum gas injection systems are among the most popular. It becomes necessary to know mathematical descriptions of the opera-tion of individual components. The article presents a mathematical model that describes the operation of the low-pressure gas injector. Valtek plunger injector was chosen as the test object. The mathematical description includes three parts, i.e. electric, mechanical and pneumatic. The electrical part describes the generation of electromagnetic force by a circuit with a coil, in the mechanical equilibrium equa-tion of forces acting on the plunger, and in the pneumatic part the air pressure on the plunger. The calculations were performed in the Matlab/Simulink environment, creating current waveforms, acting forces and plunger displacement. Correctness of mathematical descrip-tion and determined in the course of opening and closing time calculations were related to the values declared by the manufacturer, show-ing differences below 3%. The presented mathematical model can be modified for other injector design solutions.

Key words: Mechanical Engineering, Combustion Engines, Alternative Fuel Supply, Modelling

1. INTRODUCTION

In recent years, natural oil deposits have been exploited at a rapid rate, resulting in rising fuel prices on international markets, and consequently, the number of engines powered by alternative liquefied petroleum gas (LPG) is growing year on year. (Raslavičius et al., 2014). The use of LPG as a fuel dates back to the beginning of the 20th century, and with the development of motorisation, the popularity of this fuel is growing. Manufacturers of gas systems and their components are required to meet the homologation requirements. Regardless of the original fuel system (carburettor, direct and indirect injection) or general trends like downsizing (Leduc et al., 2003), the alternative fuel supply must meet the emission requirements at the point of homologation (Ristovski et al., 2005; Mustafa and Gitano-Briggs, 2009). The problem is the successive tightening of emission standards for internal combustion engines used in transport (Bielaczyc and Woodburn, 2018), non-road and working machines (Waluś et al., 2018; Warguła et al., 2020). The tightening of emission standards is accompanied by changes in the organisation of driving tests (Bielaczyc and Woodburn, 2018). This forces manufacturers to constantly search for new solutions in the structure of the combus-tion process (Onishi et al., 1979; Jeuland et al., 2004; Mikulski et al., 2018) or the drive sources (Dimitrowa and Marechal, 2015; Grigor`ev et al., 2015; Raslavičius et al., 2017; Simon, 2017).

The required condition for proper operation of the gas injection system is evenness (Szpica, 2018a) and repeatability (Szpica, 2018) of injector dosage. In order to properly dose the fuel, injec-tors with specific flow parameters, operation delay and durability are required (Czarnigowski, 2012; Borawski, 2015). Therefore, already in the course of construction, the gas injector should meet certain requirements, and mathematical modelling should be used for preliminary tests.

There is a growing interest in computational methods that al-low testing virtual prototypes of new solutions. The possibilities of solving mathematical dependencies, similarly as in general tech-nical issues, are searched for using dedicated software for analyt-ical or numerical calculations (Mieczkowski et al., 2007; Mikulski et al., 2015; Marczuk et al., 2019; Brumercik et al., 2020). An alternative to this procedure is to use specialised software based on finite element method (FEM) (Bensetti et al., 2006; Cheng et al., 2014; Mieczkowski et al., 2020) or computational fluid dynam-ics (CFD) (Wendeker et al., 2007; Czarnigowski et al., 2009). Similarly, with the modelling of the working cycle of an LPG en-gine, it can be solved in an analytical (Cao et al., 2007) or numeri-cal (Pulawski and Szpica, 2015) way.

The fuel injector in its mathematical description focuses on many aspects. In the execution part, there is a coil with a circuit generating electromagnetic field causing valve movement (Passa-rini and Nakajima, 2003; Passarini and Pinotti, 2003) or piezoelec-tric drive (Pogulayev et al., 2015; Mieczkowski, 2019; Mieczkow-ski, 2019a). In the mechanical part, the motion of the actuator element is analysed (Lim et al., 1994) and related to friction (Borawski, 2018, 2019) along with aerodynamic drag. Hydraulic aspects concern the process of flow through the cycle working valve (Czarnigowski et al., 2007; Marčič et al., 2015). A separate part in modelling of the fuel injector operation process is formed by the issues of electric power supply. The specificity of the signal controlling the opening of the fuel injector is based on a transistor key, which is also designed to limit the power supply to prevent overheating of the injector (Hung and Lim, 2019). For this pur-pose, a pulse-width modulation (PWM) signal is used some time after the opening is initiated (Taghizadeh et al., 2009; Szpica, 2016). Each time a fuel injector is modelled, input data is required to determine the geometry, electrical, mechanical or hydraulic processes.

Due to the lack of a comprehensive mathematical model de-scribing the operation of the low-pressure gas injector, an attempt

was made to create it. Considering some limitations, especially in the mathematical description of the electromagnetic field generated by the coil with moving core, an empirical model was proposed. The goal was also to show the influence of particular factors shaping plunger displacement. On this basis, the factors of minor importance may be omitted in the course of model simplification. The presented approach allows to develop, based on the proposed mathematical description, models of varying degrees of complexity and possible extensions.

2. THE RESEARCH OBJECT

The object of the research was Valtek Rail Typ 30 low pressure gas injector (Fig. 1). This is a plunger type injector with a transverse flow. The plunger movement is caused by an electromagnetic circuit that includes coil and cramp. The spring is responsible for plunger contact with the corps at standstill. The plunger movement is bounded by a limiter. The gas flows from the inlet nozzle to the outlet nozzle when the coil is electrically powered and the plunger is moved. The plunger has elastic feet mounted at the bottom and top.
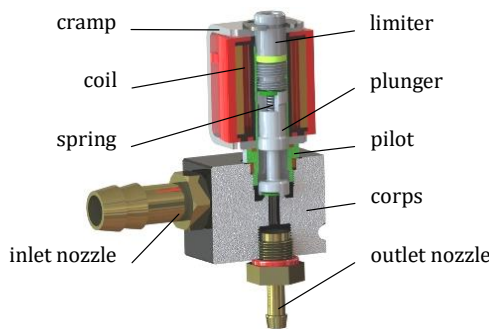
Fig. 1. Valtek Rail Typ 30 gas injector

Basic technical data of the Valtek injector have been presented in Table 1.

Tab. 1. Basic technical data of the Valtek Rail Typ 30 gas injector (https://www.valtek.it/...)

Parameter	Unit	Value
Coil resistance	Ω	3
Plunger displacement	mm	0.4
Nozzle size	mm	Min. 1.5 / Max. 3.5
Opening time	ms	3.4
Closing time	ms	2.2
Max. working pressure	Pa	4.5 $e5$

3. MODELLING METHODOLOGY

The mathematical modelling of the low-pressure gas injector can be based on mathematical descriptions of electrovalves from pneumatic actuators (Rahman et al., 1996a, 1996b; Chu et al., 2007; Kamiński, 2013, 2014) or liquid fuel injectors. In case of fuel injectors, the models can be divided into physical zero, single or multi-dimensional (Matković et al., 2005; Czarnigowski et al., 2007; Ouyang, 2009; Minghai and Feng, 2010; Li and Jiang,

2010) and empirical (Duk and Czarnigowski, 2001; Mehlfeldt et al., 2008; Yang et al., 2012, Borawski, 2015a). The issues mainly concern the movement of the injector's execution element, which in effect determines the mass of fuel that flows out of it (Morselli et al., 2002; Mehlfeldt et al., 2008; Liu and Ouyang, 2009; Li and Jiang, 2010; Haiping and Xianyi, 2010). All mathematical models emphasise the existence of time delays resulting mainly from inertia forces and resistance to motion of the executive element in the ratio of a given impulse to fuel outflow (Szpica, 2017).

The mathematical description of the function of the low-pressure gas injector is based on Fig. 2.
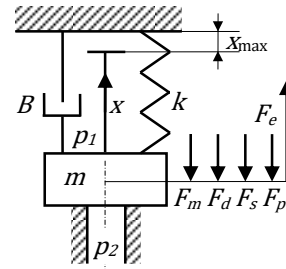
Fig. 2. The scheme of the gas injector (description in the main text)

Due to the high complexity of the mathematical description, the following simplifying approaches were assumed:
- the plunger movement is caused by the result of acting forces (the reflection effect in the return positions is omitted);
- body vibrations and other mechanical disturbances do not affect the plunger movement;
- eddy currents, magnetic saturation and coil temperature do not affect the parameters of the electromagnetic circuit;
- the pressing force coming from the air pressure depends on the plunger position;
- friction is divided into static, kinetic and viscous and its value depends on plunger movement (coefficient values do not depend on temperature and pressure inside the body);
- the aerodynamic drag force of the plunger is included;
- due to the complexity of construction, the inductance of the electromagnetic circuit will be determined experimentally;
- stiffness of the pressure spring will be determined experimentally, vibrations will be omitted.

The equation of equilibrium on this basis (Fig. 2) can be written down in the form:

$$F_m + F_d + F_s + F_p = F_e \qquad (1)$$

where F_m is the resistance force of mass inertia, F_d the friction force, F_s the spring force, F_p the pressure force and F_e is the electromagnetic force.

The resistance force of mass inertia in reciprocating motion inertial force is described as:

$$F_m = m \frac{\mathrm{d}^2 x}{\mathrm{d}t^2} \qquad (2)$$

where m is the mass of the moving element.

In the case of injector plunger movement, damping (B in Fig. 2) may be the result of friction between plunger and corps as well as gas and aerodynamic drag force. Despite the fact that the electromagnetic system should align the plunger, it is assumed that under horizontal mounting conditions, the plunger will press its weight on the pilot.

The damping force is described as:

$$F_d = \begin{cases} F_{fs} & \text{if } x = 0, x = m_{\max} \\ F_{fk} + F_v + F_{df} & \text{if } x \neq 0 \end{cases} \quad (3)$$

where $F_{fs} = \mu_s F_N$ is the force of static friction, F_N the normal force, $F_{fk} = \mu_k F_N$ the force of kinetic friction, $F_v = \mu_v \frac{dx}{dt} \text{sgn}(x)$ the force of viscous friction, $F_{df} = 0.5 A c_d \rho v^2 \text{sgn}(x)$ the force of aerodynamic drag, μ_s the coefficient of static friction, μ_v the coefficient of viscous friction, μ_k the coefficient of kinetic friction, c_d the drag coefficient, ρ the density of air, $v = \frac{dx}{dt}$ the flow velocity and A is the characteristic frontal area of the body.

The spring force is described as:

$$F_s = k(x_0 + x) \quad (4)$$

where k is the spring stiffness, x the displacement element and x_0 is the initial tension of the spring.

The pressure force is given as:

$$F_g = \begin{cases} A_1 p_1 + A_2 p_2 & \text{if } x = 0 \text{ mm} \\ 0 & \text{if } x > 5e - 7 \text{ mm} \end{cases} \quad (5)$$

where A_1 is the cross area over the valve, p_1 the gas pressure, A_2 the cross area under the valve and p_2 is the inlet manifold pressure.

The electromagnetic force being the result of the circuit operation can be obtained from the relation:

$$F_e = \frac{1}{2} I^2 \frac{dL(x)}{dx} \quad (6)$$

where I is the current and L is inductance.

Using the Faraday`s and Kirchhoff`s laws, one may obtain a differential equation describing the change of the current supplying the electromagnetic circuit:

$$\frac{dI}{dt} = \frac{1}{L(x)}\left(U - RI - \frac{dL(x)}{dx}\frac{dx}{dt}I\right) \quad (7)$$

where R is the resistance and U is the voltage.

Then, substituting all components to Eq. 1, we will obtain an equation of equilibrium that is as follows:

$$a = \frac{dv}{dt} = \frac{F_e - F_m - F_d - F_s - F_p}{m} \quad (8)$$

To solve Eq. 8, numerical methods are used and a dedicated software is needed. The calculation process is dependent on the values of input parameters and boundary conditions. There are two options to deal with boundary conditions. In the first simpler variant, hard plunger displacement limits are defined (Borawski, 2015a) in the second variant, it is necessary to describe meticulously mechanical collisions (Tian and Zhao, 2018). The hard constraints are realised by the correct setting of the integrating integrator, while the description of mechanical collisions is a complex system of switch commands. The second variant also allows for more precise modelling of the plunger rebound event in the turning positions.

4. NECESSARY PARAMETER TO INITIATE CALCULATION

In case of controlling the opening of the gas injector, a transistor key is used and the voltage course is specific for the so-called short to ground (Szpica, 2018b). Therefore, this type of extortion should be reversed as an input value in the model, bypassing the part of the voltage drop, where overvoltage occurs in the opposite direction to extortion. Finally, the extortion signal is defined as a rectangle with the height equal to the value of the supply voltage and the length resulting from the opening time.

One of the most important parameters required to initiate calculations is the relation between the inductance of the electromagnetic system and the plunger displacement. There are many analyses in the literature to calculate this parameter dependent on coil parameters and installation geometry. The calculations are based on empirical and numerical models (Pacurar et al., 2015; Bali and Erzan Topcu, 2018). The studies mainly focus on air coils without considering the internal core movement (Lu and Jensen, 2003; Xiang et al., 2008; Plavec et al., 2019; Taghizadeh et al., 2009; Dongiovanni and Coppo, 2010; Cheng et al., 2015). In mathematical descriptions that take into account the movable core, there is no clear experimental verification (Cheung at al., 1993; Cvetkovic et al., 2008; Liu et al., 2011; Lunge and Kurode, 2013; Li et al., 2017; Tian and Zhao, 2018; Demarchi et al., 2018). There are no guidelines for determining the inductance of an electromagnetic circuit, taking into account the construction conditions and characteristics of the materials used.

This is why it was decided to use the results of the experimental research included in Szpica (2016a). The values were measured RLC CMT-417 Meter and a special test will be used at 100 Hz pulse frequency. The measurement results are presented in Fig. 3. The relation $L = f(x)$ was approximated with the polynomial of 3rd degree achieving the compliance, which is confirmed by the value $R^2 = 99.9$ %. On the result of the approximation dependence, a derivative was determined:

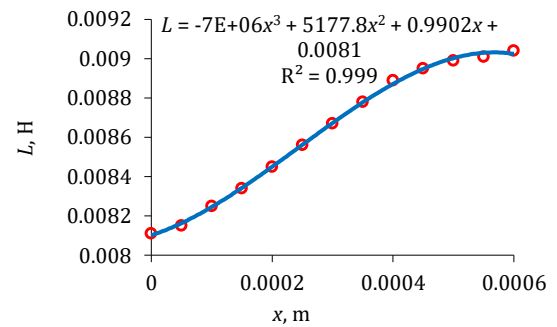$$\frac{dL(x)}{dx} = -21e6x^2 + 10355.6x + 0.990 \quad (9)$$

Fig. 3. Test results on inductance as a function of the lift of the injector working component

Due to the complicated shape of the pressure spring, its rigidity was determined experimentally. For this purpose, the AXIS FB50 50 N with tripod and MITUTOYO altimeter was used, as well as the measuring range including working stroke and preload. The measurement results are presented in Fig. 4. The trend line was linearly approximated to a stiffness of 832.83 N/m ($R^2 = 99.9$ %).

The parameters needed to initiate the simulation have been presented in Table 2. At the input, the voltage control pulse was set in the form of a rectangular run. At $t = 0$ s, the voltage reached $U = 12$ V and the plunger was in the position $x = 0$ m. After the time $t = t_{inj}$, the voltage dropped in steps to $U = 0$ V. The integrating integrator of displacements had been set to a limit value of $x_{\max}$.
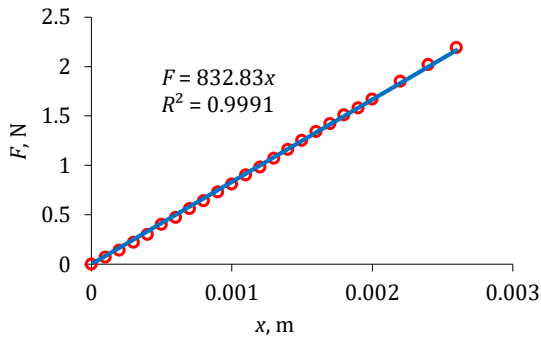
Fig. 4. Test results on the spring stiffness

Tab. 2. Parameters, functions and conditions needed to initiate the simulation

Parameter	Volume
Injection time	$t_{inj} = 5$ ms
Mass of the piston and needle	$m = 5e-3$ kg
Resistance	$R = 3 \, \Omega$
Inductance function	Fig. 3 and Eq. 9
Spring stiffness	Fig. 4
Initial tension the spring	$x_0 = 0.75$ mm
Coefficient of static friction	$\mu_s = 0.61$
Coefficient of kinematic friction	$\mu_k = 0.47$
Coefficient of viscous friction	$\mu_v = 0.009$ Ns/m
Coefficient of aerodynamic drag	$c_d = 1$
Normal force	$F_N = m \, g$
Characteristic frontal area of the body, cross area over the valve	$A = A_1 = 32.56e-6$ m^2
Cross area under the valve	$A_2 = 12.56e-6$ m^2
Gas pressure	$p_1 = 1e5$ Pa $+ p_2$
Inlet manifold pressure	$p_2 = 1e5$ Pa
Density of air	$\rho = 1.2$ kg/m^3

5. RESULTS OF THE SIMULATION

By twice integrating the relation Eq. 8, we will obtain a displacement of the piston. It allows conducting calculations of the gas injector operation in the entire cycle, i.e. opening, holding the open position and closing. The differential Eq. 8 was solved numerically with the implicit trapezoidal method combined with reverse differentiation (variable steps, min. step $1e-7\,s$) in Matlab/Simulink (Yang et al., 2005). This software allows for easy implementation of empirical models in workspace, which has been confirmed in studies (Shamdani et al., 2006; Borawski, 2015a; Demarchi et al., 2018).

As a result of the simulations, it is possible to evaluate the correctness of the mathematical description on the basis of the voltage U, current I and displacement x (Fig. 5).

Analysing the course in Fig. 5, it can be seen that the injector starts opening with a delay of $t_{ro} = 2.17$ ms and the opening process itself takes $t_o = 1.30$ ms. The current course is visible when the injector reaches complete opening. After a power cut, the injector closes. The exact time to fully open $t_{fo} = 3.47$ ms and to fully close $t_{fc} = 2.15$ ms is read from the graph.
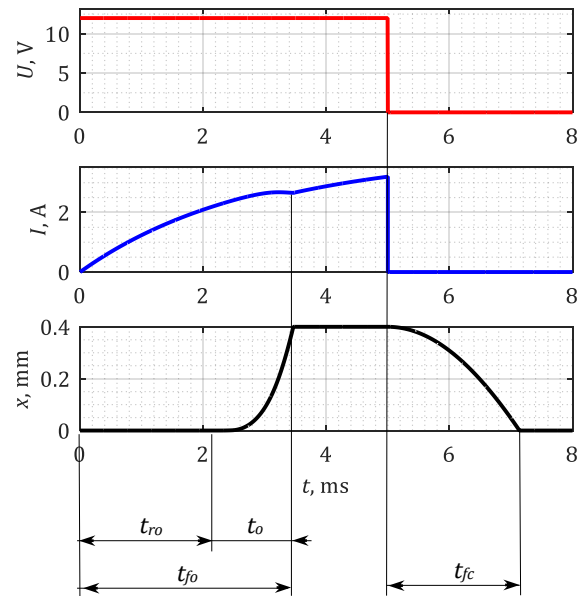

Fig. 5. The results of the simulation: t_{ro} – opening response times, t_o – opening times, t_{fo} – full opening times, t_{fc} – full closing times

Presented in Eq. 1 the balance of forces acting on the plunger determines its movement. As can be seen in Fig. 6, the initial phase of the injector's operation marked as A is the overcoming by the electromagnetic force F_e of air pressure F_p, spring force F_s and static friction force F_{fs}.
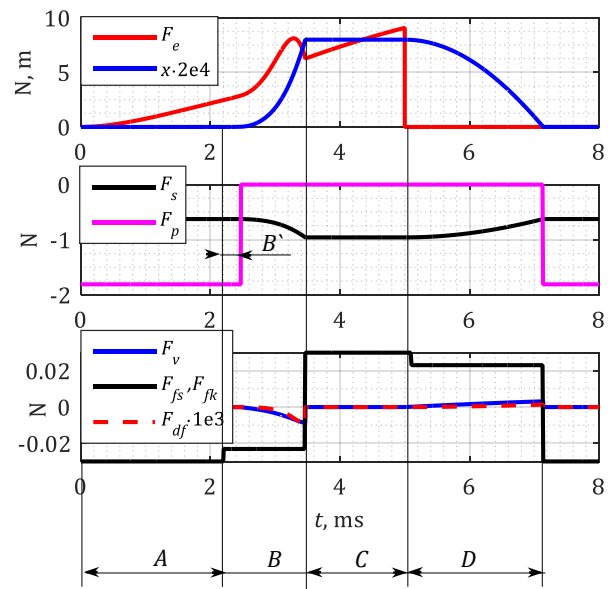

Fig. 6. Course of the forces and displacement (description in the main text)

At the start of the movement, the static friction force F_{fs} changes into the kinetic friction force F_{fk}, and after time $B`$, the force F_p disappears. During the displacement of the plunger (B in Fig. 6), the viscous friction force F_v and the aerodynamic drag force F_{df} are added as load, which change their turn in the return motion, just like F_{fk}, and the plunger inertia. In section C, only the

electromagnetic force increases because the plunger is stationary. At closure (D in Fig. 6), the spring's stiffness is responsible for the return motion, and it determines this process, since the electromagnetic force F_e fades away in steps. To sum up Fig. 6, it should be stated that the dominant forces are the electromagnetic force F_e, the air pressure force F_p, the spring force F_s and the plunger inertia. The remaining forces have little influence on the opening and closing process of the injector, especially the viscous friction force F_v and the aerodynamic drag force F_{df}.

The injector opening and closing times calculated in the course of analysis were compared with those declared by the manufacturer (Table 3). It was found that full opening time differs by 2.05 % and full closing time by 2.27 % from the manufacturer's declaration, which should be considered an acceptable result. In the case of the opening process, the reason for this difference can be assumed to be the acceptance of a force loss in steps from the pressure F_p to the set value of the lift x. In addition, the inductance was determined at a certain frequency, which may also affect the calculation results. In the case of the closing process, the power cut may have been influenced by the power drops, which, however, fall with some slight delay (Szpica, 2017).

Tab. 3. The technical data and calculated comparison

Parameter	Technical data (ms)	Calculated (ms)	Absolute error (%)
Full opening time	3.40	3.47	2.05
Full closing time	2.20	2.15	2.27

In the course of further activities, it is planned to implement the model presented in the study to other injector design solutions, including plate and membrane. In these cases, the model descriptions of electromagnetic circuits available in the literature should be considered more accurately. Additionally, it is planned to develop a mathematical model of the electromagnetic circuit, which can be used in modelling of the operation of the low pressure gas injector without the need for experimental determination. The final requirement will be to carry out an experimental validation of the simulation results using sensors that do not interfere with the injector's electromagnetic field generating system.

6. CONCLUSIONS

The article describes the course of mathematical modelling of the low-pressure gas injector. The overall mathematical model consists of several parts: electrical, mechanical and hydraulic. In the electrical part, the process of rising and falling of the supply current depending on the supply voltage and magnetic properties of the circuit with the coil is described. In the mechanical part, inertia and frictional resistances and aerodynamics are taken into account, also taking into consideration the spring return pressure. Hydraulic part is the pressure force on the plunger coming from the air pressure, which is assumed in the model as the working medium. The calculations were carried out in the Matlab/Simulink environment, and the Valtek Rail Type 30 injector was selected as the object.

On the basis of the work carried out, the following conclusions can be made :

– The proposed mathematical description of the operation of the low-pressure gas injector allows to simulate its operation.

– The use of experimental results and their implementation into an empirical model seems to be useful in modelling a complex electromagnetic system with a coil and a movable core.

– The movement of the working element of the gas injector (plunger) is determined by the electromagnetic force, inertia, pressure and spring.

– Little influence of frictional and aerodynamic drag on the process of opening and closing the gas injector has been noticed.

– The results showed that full opening time differs by 2.05 % and full closing time by 2.27 %, which gives grounds to consider the proposed model to be correct.

Some imperfections in the mathematical description were noticed which may influence the results. This is a reason for further mathematical analyses and the necessity to carry out partial experimental research, i.e. electromagnetic force acting on the plunger, frictional resistances and others.

REFERENCES

1. **Bali E., Erzan Topcu E.** (2018), Design of on-off type solenoid valve for electropneumatic brake system and investigation of its statistics characteristics, *International Journal of Advances on Automotive and Technology*, 2(3): 175–184.
2. **Bensetti M., Bihan Y.L., Marchand C.** (2006), Development of an hybrid 3D FEM for the modeling of micro-coil sensors and actuators, *Sensors and Actuators A: Physical*, 129(1): 207–211.
3. **Bielaczyc P., Woodburn J.** (2018), Trends in automotive emissions legislation: impact on LD engine development, fuels, lubricants, and test methods - a global view, with a focus on WLTP and RDE regulations - Summary of the 6th International Exhaust Emissions Symposium (IEES), *Combustion Engines*, 174(3): 56–65
4. **Borawski A.** (2015), Modification of a fourth generation LPG installation improving the power supply to a spark ignition engine, *Eksploatacja i Niezawodnosc – Maintenance and Reliability*, 17(1): 1–6.
5. **Borawski A.** (2015a), Simulation studies of LPG injector used in 4th generation installations, *Combustion Engines*, 160(1): 49–55.
6. **Borawski A.** (2018). Simulation Study of the Process of Friction in the Working Elements of a Car Braking System at Different Degrees of Wear. Acta Mechanica et Automatica, 12(3): 221–226.
7. **Borawski A.** (2019), Common methods in analysing the tribological properties of brake pads and discs - a review, *Acta Mechanica et Automatica*, 13(3): 189–199.
8. **Brumercik F.; Lukac M.; Caban J. Krzysiak Z.; Glowacz A.** (2020), Comparison of selected parameters of a planetary gearbox with involute and convex–concave teeth flank profiles, *Applied Science*, 10: 1417.
9. **Cao Y., Teng W., Zhang H.** (2007), Dynamic modeling and hardware-in-the-loop simulation testing for LPG engine, *Proceedings of the 2007 IEEE International Conference on Mechatronics and Automation*, 2093–2098.
10. **Cheng Q., Zhang Z.-D., Guo H., Xie N.-L.** (2015), Electro-magnetic-thermal coupling of GDI injector, *Journal of Jilin University (Engineering and Technology Edition)*, 45(3): 806–813
11. **Cheng Q., Zhang Z-D., Guo H., Xie N-L.** (2014), Simulation and analysis on electro-magnetic-thermal coupling of solenoid GDI injector, *International Journal of Applied Electromagnetics and Mechanics*, 46(4): 775–792.
12. **Cheung N.C., Lim K.W., Rahman M. F.** (1993), Modelling a linear and limited travel solenoid, *Proceedings of IECON '93 - 19th Annual Conference of IEEE Industrial Electronics*, 3: 1567–1572.
13. **Chu L., Hou Y., Liu M., Li J., Gao Y., Ehsani M.** (2007), Study on the dynamic characteristics of pneumatic ABS solenoid valve for commercial Vehicle, *2007 IEEE Vehicle Power and Propulsion Conference*, 641–644.

14. **Cvetkovic D, Cosic I., Subic A.** (2008), Improved performance of the electromagnetic fuel injector solenoid actuator using a modelling approach, *International Journal of Applied Electromagnetics and Mechanics*, 27: 251–273.

15. **Czarnigowski J.** (2012), *Teoretyczno-empiryczne studium modelowania impulsowego wtryskiwacza gazu*, Wydawnictwo Politechniki Lubelskiej, Lublin.

16. **Czarnigowski J., Jaklinski P., Wendeker M., Pietrykowski K., Gabowski Ł.** (2009), The analyses of the phenomena inside a CNG flap-valve injector during gas flow. *Combustion Engines*, 1(136): 10–18.

17. **Czarnigowski J., Wendeker M., Jakliński P., Rola M., Grabowski Ł., Pietrykowski K.** (2007), CFD model of fuel rail for LPG systems, *JSAE/SAE International Fuels & Lubricants Meeting*, 2007-01-2053.

18. **Demarchi A., Farçoni L., Pinto A., Lang R., Romero R., Silva I.** (2018), Modelling a solenoid's valve movement, In: Akiyama H., Obst O., Sammut C., Tonidandel F. (eds) *RoboCup 2017: Robot World Cup XXI. RoboCup 2017. Lecture Notes in Computer Science*, Cham: Springer, 11175.

19. **Dimitrova Z., Maréchal F.** (2015), Gasoline hybrid pneumatic engine for efficient vehicle powertrain hybridization, *Applied Energy*, 151: 168–177.

20. **Dongiovanni C., Coppo M.** (2010), *Accurate Modelling of an Injector for Common Rail Systems*. In book: Siano D. *Fuel Injection*, London: IntechOpen Limited, 6: 95–119.

21. **Duk M., Czarnigowski J.** (2001), The method for indirect identification gas injector opening delay time, *Przeglad Elektrotechniczny*, 88(10b): 59–63.

22. **Grigor'ev M.A., Naumovich N.I., Belousov E.V.** (2015), A traction electric drive for electric cars, *Russian Electrical Engineering*, 86(12): 731–734.

23. **Haiping Y., Xianyi Q.** (2010), The calculation of main parameters of the gasoline engine fuel injection system, *Proceeding of the International Conference on Computer Application and System Modeling (ICCASM)*, V13–635.

24. **Hung N.B., Lim O.T.** (2019), Improvement of electromagnetic force and dynamic response of a solenoid injector based on the effects of key parameters, *International Journal of Automotive Technology*, 20: 949-960.

25. **Jeuland N., Montagne X., Duret P.** (2004), New HCCI/CAI combustion process development: Methodology for determination of relevant fuel parameters, *Oil & Gas Science and Technology*, 59(6): 571–579.

26. **Kamiński Z.** (2013), Experimental and numerical studies of mechanical subsystem for simulation of agricultural trailer air braking systems, *International Journal of Heavy Vehicle System*, 20(4): 289–311.

27. **Kamiński Z.** (2014), Mathematical modelling of the trailer brake control valve for simulation of the air brake system of farm tractors equipped with hydraulically actuated brakes, *Eksploatacja i Niezawodnosc – Maintenance and Reliability*, 16(4): 637–643.

28. **Leduc L., Dubar B., Ranini A., Monnier G.** (2003), Downsizing of gasoline engine: an efficient way to reduce CO2 emissions. *Oil & Gas Science Technology*, 58(1): 115–127.

29. **Li P.X., Su M., Zhang D.B.** (2017), Response characteristic of high-speed on/off valve with double voltage driving circuit, *IOP Conference Series: Materials Science and Engineering*, 220: 012028.

30. **Lim K.W., Cheung N.C., Kahman M.F.** (1994), Proportional control of a solenoid actuator, *Proceedings of IECON'94 - 20th Annual Conference of IEEE Industrial Electronics*, 2045–2050.

31. **Liu Y.-F., Dai, Z.-K., Xu X.-Y., Tian L.** (2011), Multi-domain modeling and simulation of proportional solenoid valve, *Journal of Central South University Technology*, 18: 1589–1594.

32. **Liu Z., Ouyang G.** (2009), Numerical analysis of common rail electro-injector for diesel engine, *Proceedings of the International 2009 Conference on Mechatronics and Automation (IEEE)*, 1683–1688.

33. **Lu F., Jensen D.** (2003), Potential viability of a fast-acting micro-solenoid valve for pulsed detonation fuel injection, *41st Aerospace Sciences Meeting and Exhibit, Aerospace Sciences Meetings*, 2003-0888.

34. **Lunge, S.P., Kurode S.R.** (2013), Proportional actuator from on off solenoid valve using sliding modes, *Proceedings of the 1st International and 16th National Conference on Machines and Mechanisms (iNaCoMM2013)*, 1020–1027.

35. **Marčič S., Marčič M., Praunseis Z.** (2015), Mathematical Model for the Injector of a Common Rail Fuel-Injection System. *Engineering*, 7: 307–321.

36. **Marczuk A., Caban J., Aleshkin A.V., Savinykh P.A., Isupov A.Y., Ivanov I.I.** (2019), Modeling and simulation of particle motion in the operation area of a centrifugal rotary chopper machine, *Sustainability*, 11(18): 1–15.

37. **Matković K., Jelović M., Jurić J., Konyha Z., Gračanin D.** (2005), Interactive visual analysis and exploration of injection system simulations, *Proceedings of the International Conference on Vizualization (VIS 05. IEEE)*, 391–398.

38. **Mehlfeldt D., Weckenmann H., Stöhr G.** (2008), Modeling of piezoelectrically actuated fuel injectors, *Mechatronics*, 18: 264–272.

39. **Mieczkowski G.** (2019), Criterion for crack initiation from notch located at the interface of bi-material structure, *Eksploatacja i Niezawodnosc – Maintenance and Reliability*, 21 (2): 301–310.

40. **Mieczkowski G.** (2019a), Static electromechanical characteristics of piezoelectric converters with various thickness and length of piezoelectric layers, *Acta Mechanica et Automatica*, 13(1): 30–36.

41. **Mieczkowski G., Borawski A., Szpica D.** (2020), Static electromechanical characteristic of a three-layer circular piezoelectric transducer, *Sensors*, 20, 222.

42. **Mieczkowski G., Molski K., Seweryn A.** (2007), Finite-element modeling of stresses and displacements near the tips of pointed inclusions, *Materials Science*, 43(2): 183–194.

43. **Mikulski M., Balakrishnan P.R., Doosje E., Bekdemir C.** (2018), Variable valve actuation strategies for better efficiency load range and thermal management in an RCCI engine, *SAE Technical Papers*, 2018-01-0254.

44. **Mikulski M., Wierzbicki S., Piętak A.** (2015), Numerical studies on controlling gaseous fuel combustion by managing the combustion process of diesel pilot dose in a dual-fuel engine, *Chemical and Process Engineering*, 36(2): 225–238.

45. **Li M.H., Jiang F.** (2010), Simulation research on fuel injection system of 16V265H Dielsel engine introduced from U.S., *Proceedings of the International Conference on E-Product E-Service and E-Entertainment (ICEEE)*, 4796–4799.

46. **Morselli R., Corti E., Rizzoni G.** (2002), Energy based model of a common rail injector, *Proceeding of the International Conference on Control Applications (IEEE)*, 2: 1195–1200.

47. **Mustafa K.F., Gitano-Briggs H.W.** (2009), Liquefied petroleum gas (LPG) as an alternative fuel in spark ignition engine: Performance and emission characteristics. *Proceedings of the International Conference Energy and Environment (ICEE)*, 189–194.

48. **Onishi S., Jo S.H., Shoda K., Jo P.D., Kato S.** (1979), Active thermo-atmosphere combustion (A.T.A.C.) - A new combustion process for internal combustion engines, *SAE Paper*, 790501.

49. **Pacurar C., Topa V., Munteanu C., Racasan A., Hebedean C., Oglejan R., Vlad G.** (2015), Solenoid actuator parametric analysis and numerical modeling, *Acta Electrotehnica*, 56(3): 246–251.

50. **Passarini L.C., Nakajima P.R.** (2003), Development of a high-speed solenoid valve: an investigation of the importance of the armature mass on the dynamic response, *Journal of the Brazilian Society of Mechanical Sciences and Engineering*, XXV(4): 329–335.

51. **Passarini L.C., Pinotti JR, M.** (2003), A new model for fast-acting electromagnetic fuel injector analysis and design, *Journal of the Brazilian Society of Mechanical Sciences and Engineering*, 25(1): 95–106.

52. **Plavec E., Ladisic I., Vidovic M.** (2019), The impact of coil winding angle on the force of DC solenoid electromagnetic actuator, *Advances in Electrical & Electronic Engineering*, 17(3): 244–250.

53. **Pogulyaev Y.D., Baitimerov R., Rozhdestvensky Y.** (2015), Detailed dynamic modeling of common rail piezo injector, *Procedia Engineering*, 129: 93–98.

54. **Pulawski G., Szpica D.** (2015), The modelling of operation of the compression ignition engine powered with diesel fuel with LPG admixture, *Mechanika*, 21(6): 501–506.

55. **Rahman M. F., Cheung N. C., Lim K. W.** (1996a), Converting a switching solenoid to a proportional actuator, *IEEJ Transactions on Electrical and Electronic Engineering*, I-16(5): 531–537.

56. **Rahman M. F., Cheung N. C., Lim K. W.** (1996b), Modeling of a nonlinear solenoid toward the development of a proportional actuator, *Procceedings of the 5th International Conferences Modeling and Simulation of Electrical Machines Convertors and Systems ELECTRIMACS'96*, 2: 695–670.

57. **Raslavičius L., Keršys A., Makaras R.** (2017), Management of hybrid powertrain dynamics and energy consumption for 2WD, 4WD, and HMMWV vehicles, *Renewable and Sustainable Energy Reviews*, 68(1): 380–396.

58. **Raslavičius L., Keršys A., Mockus S., Keršiene N., Starevičius M.** (2014), Liquefied petroleum gas (LPG) as a medium-term option in the transition to sustainable fuels and transport, *Renewable & Sustainable Energy Reviews*, 32: 513–525.

59. **Ristovski Z.D., Jayaratne E.R., Morawska L., Ayoko G.A., Lim M.** (2005), Particle and carbon dioxide emissions from passenger vehicles operating on unleaded petrol and LPG fuel, *Science of the Total Environment*, 345: 93–98.

60. **Shamdani, A.H., Shamekhi, A.H., Basharhagh, M.Z.** (2006). Modeling and Simulation of a Diesel Engine Common Rail Injector in Matlab/Simulink, *14th Annual (International) Mechanical Engineering Conference*, 7.

61. **Simon M.** (2017), Pneumatic vehicle, research and design, *Procedia Engineering*, 181: 200–205.

62. **Szpica D.** (2016), Modeling of current limitation through the PWM signal in LPG injectors, *Proceedings of 20th International Scientific Conference Transport Means 2016*, 536–539.

63. **Szpica D.** (2016a), Testing the parameters of LPG injector solenoids as a function of the lift of the working component and the frequency of impulses, *Proceedings of 20th International Scientific Conference Transport Means 2016*, 551–555.

64. **Szpica D.** (2017), Comparative analysis of low pressure gas-phase injector's characteristics, *Flow Measurement and Instrumentation*, 58: 74–86.

65. **Szpica D.** (2018), Investigating fuel dosage non-repeatability of low pressure gas-phase injectors, *Flow Measurement and Instrumentation*, 59: 147–156.

66. **Szpica D.** (2018a), Research on the influence of LPG/CNG injector outlet nozzle diameter on uneven fuel dosage, *Transport*, 33(1): 186–196.

67. **Szpica D.** (2018b), Validation of indirect methods used in the operational assessment of LPG vapor phase pulse injectors, *Measurement*, 118: 253–261.

68. **Taghizadeh M, Ghaffari A, Najafi F.** (2009), Modeling and identification of a solenoid valve for PWM control applications, *Comptes Rendus Mecanique*, 337(3): 131–140.

69. **Tian H, Zhao Y.** (2018), Coil inductance model based solenoid on/off valve spool displacement sensing via laser calibration. *Sensors*, 18(12): 4492.

70. Valtek Type 30 – technical data. [online] [02.08.2018]. Available at: https://www.valtek.it.

71. **Waluś K.J., Warguła Ł., Krawiec P., Adamiec J.M..** (2018), Legal regulations of restrictions of air pollution made by non-road mobile machinery - the case study for Europe: a review, *Environmental Science and Pollution Research*, 25(4): 3243–3259.

72. **Warguła Ł., Krawiec P., Waluś K.J., Kukla M.** (2020), Fuel consumption test results for a self-adaptive, maintenance-free wood chipper drive control system, *Applied Sciences*, 10(8): 2727.

73. **Wendeker M., Jakliński P., Gabowski Ł., Pietrykowski K., Czarnigowski J., Hunicz J.** (2007), Model of CNG flap valve injector for internal combustion engines, *Combustion Engines*, 4(131): 42–52.

74. **Xiang Z., Liu H., Tao G-L, Man J., Zhong W.** (2008), Development of an ε-type actuator for enhancing high-speed electro-pneumatic ejector valve performance, *Journal of Zhejiang University - Science A*, 9(11): 1552–1559.

75. **Yang L.-J., Fu Q.-F., Qu Y.-Y., Zhang W., Du M.-L., Xu B.-R.** (2012), Spray characteristics of gelled propellants in swirl injectors, *Fuel*, 97: 253–261.

76. **Yang W.Y., Cao W., Chung T.S., Morris J.** (2005), *Applied Numerical Methods Using MATLAB*; John Wiley & Sons Inc., New Jersey.